Optically injected mode-locked laser

N. Rebrova,[1] G. Huyet,[1] D. Rachinskii,[2] and A. G. Vladimirov[3]
[1]*Tyndall National Institute, Cork Institute of Technology, Ireland*
[2]*Department of Applied Mathematics, University College Cork, Ireland*
[3]*Weierstrass Institute for Applied Analysis and Stochastics, Mohrenstrasse 38, D-10117 Berlin, Germany*
(Received 8 December 2010; published 7 June 2011)

We study analytically and numerically a delay differential model of a passively mode-locked semiconductor laser subjected to a single-frequency coherent injection. The width of the locking cone is calculated asymptotically in the limit of small injection and zero line-width enhancement factors and compared to that obtained by direct numerical integration of the model equations. The dependence of the locking cone on the laser parameters is discussed.

DOI: 10.1103/PhysRevE.83.066202 PACS number(s): 05.45.Xt, 02.60.−x, 42.55.Px, 42.60.Fc

I. INTRODUCTION

Mode-locked (ML) semiconductor lasers are important devices for many applications, including optical telecommunications, optical sampling, microwave photonics, optical division multiplexing [1], and two-photon imaging [2]. Ideally, these lasers emit a periodic train of picosecond pulses with a repetition rate ranging from a few GHz to a few THz. The optical spectrum of ML lasers is commonly referred to as an optical frequency comb, where the spacing between two neighboring modes corresponds to the repetition rate of the laser. For some coherent communication or metrology applications, it is interesting to lock the position of one of the modes in the comb to an external single-frequency source. Similarly, to optically injected single mode lasers, this can be implemented using injection locking from a single-mode laser, but here the slave laser emits a frequency comb instead of a single frequency. We have recently demonstrated both theoretically and experimentally that optical injection can inhibit waveform instabilities observed in quantum dot ML lasers and improve the time-bandwidth product of these lasers [3]. Also, experiments demonstrated that a two-frequency injection can, in addition, lead to a reduction of the ML pulse-timing jitter [4].

When the frequency ν of the external injection comes sufficiently close to the frequency ν_k of one of the laser modes, the frequency of this mode locks to ν. The interval of detuning $\nu - \nu_k$, where the locking phenomenon takes place, is usually referred to as the locking range. This paper aims to estimate this range in a passively ML semiconductor laser subjected to single-frequency optical injection. Using a delay-differential equations model describing a passively ML semiconductor laser with a single-frequency optical injection, we calculate the asymptotic width of the locking range. Our simple analytical expression is in good agreement with direct numerical simulations of the full-model equations and can be considered as an analog of the formula estimating the locking range width in a cw laser subjected to a coherent optical injection [5].

The paper is organized as follows. In Sec. II, the delay differential model of an injected ML laser is presented. We discuss different regimes of the laser operation and the associated bifurcation diagrams. In Sec. III, we present results of the asymptotic analysis of the locking range in the limit of small injection amplitude and compare them with the results obtained by direct numerical integration of the model equations. We identify the domain where the asymptotic formula is in good agreement with the results of numerical simulation. Then, the dependence of the locking range on the laser parameters is discussed. Section IV contains conclusions. Derivation of the analytical results is presented in the Appendix.

II. MODEL EQUATIONS

We consider the model proposed in [6–8] for a passively mode-locked ring cavity laser with Lorentzian spectral-filtering profile and unidirectional operation. The model equations extend the classical model of Haus [9,10] to ML lasers with large gains and losses per cavity round trip, i.e., the situation typical of semiconductor lasers. After including a coherent optical injection term, the equations expressed in dimensionless variables read

$$\gamma^{-1}\frac{dA}{dt} + A = \sqrt{\kappa}\, e^{\frac{(1-i\alpha_g)G_T - (1-i\alpha_q)Q_T}{2}} A_T + \eta e^{i\omega t}, \qquad (1)$$

$$\frac{dG}{dt} = g_0 - \gamma_g G - e^{-Q}(e^G - 1)|A|^2, \qquad (2)$$

$$\frac{dQ}{dt} = \gamma_q(q_0 - Q) - s(1 - e^{-Q})|A|^2, \qquad (3)$$

where the complex variable A is the electric field envelope, the real variables G and Q describe saturable gain and loss, respectively. The dimensionless time t is related to the dimensional time t' by $t = \frac{t'}{10\text{ps}}$. The subscript T denotes time-delayed terms where the delay parameter T is the cold-cavity round-trip time. The parameter γ represents the spectral filtering bandwidth, κ is the attenuation factor describing linear nonresonant intensity losses per cavity round trip, g_0 is the pump parameter, which is proportional to the injection current in the gain region, q_0 is the unsaturated absorption parameter, γ_g and γ_q are the relaxation rates of the amplifying and absorbing sections, respectively, and s is the ratio of the saturation intensities in the gain and absorber sections. The term $\eta e^{i\omega t}$ represents optical injection with η denoting the injection strength and $\omega = 2\pi\Delta\nu$. Here $\Delta\nu = \nu - \nu_0$ measures the detuning of the frequency ν of injected light from

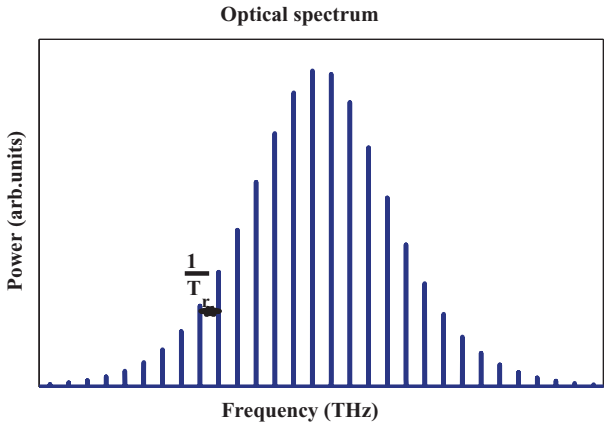

FIG. 1. (Color online) Frequency comb of the output of the mode-locked laser. $T_r \approx T$ denotes the ML pulse repetition period.

the central frequency ν_0 of the slave laser. Finally, α_g and α_q are line-width enhancement factors in gain and absorber sections. In order to simplify the asymptotic and numerical analysis, both the factors are assumed to be zero below; this simplification is discussed later in this section. Analytical and numerical study of bifurcations of the ML solution of the model equations [Eqs. (1)–(3)] without optical injection ($\eta = 0$), extensions of the model to quantum dot lasers, and comparison with other models of linear and ring-cavity lasers, have been performed in Refs. [6,11–15].

The optical spectrum of a free-running ML laser is a frequency comb with the distance between equidistant modes close to $1/T$, see Fig. 1. When the injection frequency ν is close enough to one of the modes, the slave laser locks to the external source [4]. This locking phenomenon results in a frequency shift of the entire comb by the quantity $\nu - \nu_k$, where ν_k is the modal frequency of the free-running laser closest to ν.

Figure 2 shows the central and two adjacent modes for Eqs. (1)–(3) with their locking regions obtained using the DDE-BIFTOOL software package [16]. There are three distinct areas corresponding to three different slave-laser regimes that are easily detectable experimentally. The upper area, marked CW, corresponds to the single-mode regime, i.e., when the injection strength is too large the output of the laser is a continuous wave with the angular frequency of the injected light ω. The area referred to as LML represents the values of parameters ω and η, for which the slave laser operates in ML regime and is locked to the external source. The regions denoted by letters UML correspond to the ML regimes that are not locked to the injected signal. As it is seen from Fig. 3, unlike the LML regime, which corresponds to a strictly periodic laser intensity, these regimes exhibit either quasiperiodic or irregular ML pulsations. This figure shows examples of the laser-intensity time traces calculated in different parts of the UML domain.

The bifurcation diagram shown in Fig. 2 presents domains of different laser operation regimes. The dotted line indicates the Andronov-Hopf bifurcation from the cw solution to the LML solution. The solid lines separate the domains of LML and UML solutions. Different parts of these lines correspond to the saddle-node and the Neimark-Sacker (torus) bifurca-

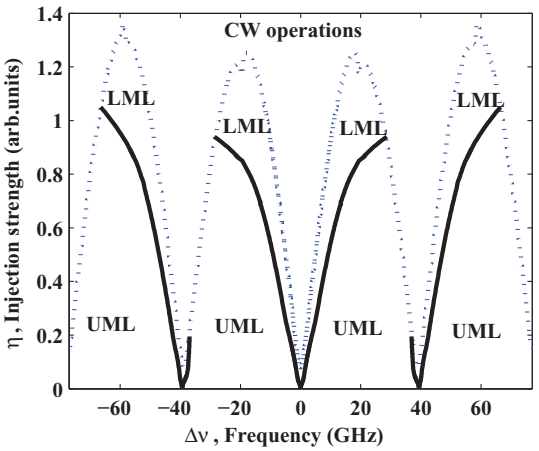

FIG. 2. (Color online) Locking regions for $\alpha_g = \alpha_q = 0$ obtained using the software package DDE-BIFTOOL. $g_0 = 1.0$, $q_0 = 2.0$, $\kappa = 0.3$, $s = 10.0$, $\gamma = 15.0$, $\gamma_g = 0.01$, $\gamma_q = 1.0$, $T = 2.5$.

tions of the LML limit cycle. A more accurate bifurcation diagram includes finer domains of more complex behavior such as multistability, harmonic regimes, chaos, etc. Detailed bifurcation analysis is, however, beyond the scope of this work as we focus on small injections into a slave laser demonstrating stable mode-locked operation.

The change of variables $A \to Ae^{i\omega t}$ transforms model Eqs. (1)–(3) to an autonomous system. A stable limit cycle $(\mathcal{A},\mathcal{G},\mathcal{Q})$ of this system with a period close to T corresponds to a fundamental ML regime of the slave laser locked to the optical-injection frequency. In the absence of injection ($\eta = 0$), the model equations are invariant with respect to an arbitrary phase shift $A \to Ae^{i\varphi}$ of the electric field amplitude. Hence, the ML regime in this case corresponds to a stable torus composed of an infinite set of neutrally stable limit cycles that are mapped one onto another by such phase shifts. The injection term breaks the phase-shift symmetry of the system. However, for small injection strength, the invariant stable torus

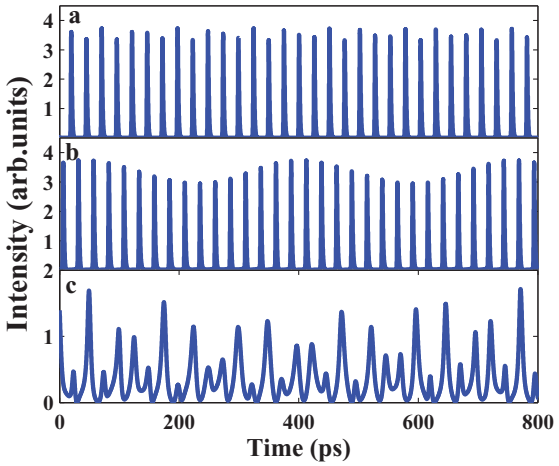

FIG. 3. (Color online) Time traces of unlocked ML (UML region on Fig. 2) solutions computed by direct numerical integration of Eqs. (1)–(3). $\alpha_g = \alpha_q = 0$, $g_0 = 1.0$, $q_0 = 2.0$, $\kappa = 0.3$, $s = 10.0$, $\gamma = 15.0$, $\gamma_g = 0.01$, $\gamma_q = 1.0$, $T = 2.5$. (a) $\eta = 0.02$, $\omega = 1$; (b) $\eta = 0.01$, $\omega = 0.4$; (c) $\eta = 0.5$, $\omega = 0.2$.

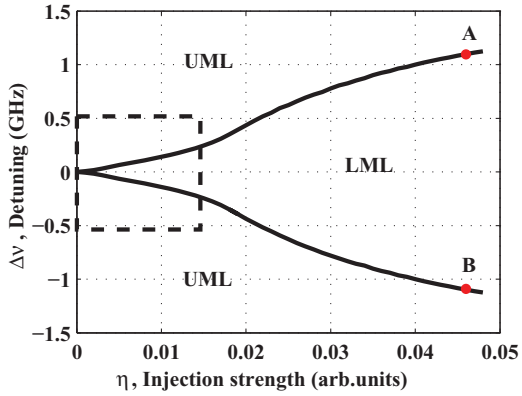

FIG. 4. (Color online) Locking cone for injections of small intensity with the frequency close to the central mode of the mode-locked regime for $\alpha_g = \alpha_q = 0$, $g_0 = 1.0$, $q_0 = 2.0$, $\kappa = 0.3$, $s = 10.0$, $\gamma = 15.0$, $\gamma_g = 0.01$, $\gamma_q = 1.0$, $T = 2.5$. The figure represents a zoom of Fig. 2 close to the origin $\Delta\nu = 0, \eta = 0$.

survives. When the detuning between the injection frequency and the frequency of one of the laser modes is sufficiently small, the dynamics on the torus is periodic; i.e., the trajectories are attracted to a stable limit cycle corresponding to the ML regime locked to the injection frequency (LML solution; Fig. 4 demonstrates the locking cone for small injections with the injection frequency close to the central mode of the slave laser). At larger detunings, this cycle collides with an unstable limit cycle in a saddle-node bifurcation (black lines separating the region LML from the regions UML in Fig. 4, and the dynamics on the invariant torus becomes quasiperiodic resulting in a ML regime that is not locked to the external signal (UML solution). The time trace of this regime is characterized by a slow periodic modulation of the pulse-peak intensity; see Fig. 3(b). For injection strengths below the codimension-two points A and B shown in Fig. 4, the locking cone (i.e., the region where the fundamental ML regime is locked to the frequency of optical injection) is bounded by two bifurcation lines corresponding to the saddle-node bifurcation of the LML limit cycle of Eqs. (1)–(3). For larger injections, the LML limit cycle destabilizes through the torus bifurcation to a regime with periodically modulated pulse-peak intensity with the increase of detuning. The saddle-node and torus-bifurcation lines meet at the codimension-two points A and B, the Gavrilov-Guckenheimer points of the Poincare map associated with the LML cycle, suggesting the presence of domains of more complex dynamics in a vicinity of these points [17].

The diagram shown in Fig. 4 is qualitatively similar to that of the injected single-mode laser, where the locking boundaries are defined by the saddle-node bifurcation of the equilibrium-locked state for small injections and the Andronov-Hopf bifurcation of this equilibrium for larger injections [18].

From Fig. 4, one can see that for small injections the width of the locking range increases almost linearly with the injection strength. This suggests that an asymptotic approach can be applied to estimate the locking range. As shown in the Appendix, in the case of zero α factors, the coefficient describing the linear expansion of the locking range can be approximated by

$$\frac{|\omega|}{\eta} \leqslant w_h, \tag{4}$$

with

$$w_h = \frac{\frac{1}{T_r}\int_0^{T_r} \psi_1^\dagger(t)\,dt}{\int_0^{T_r} \psi_1^\dagger(t)\left(\gamma^{-1}\frac{d\mathcal{A}}{dt}(t) + \mathcal{A}(t) + (\gamma T)^{-1}\mathcal{A}(t)\right)dt}, \tag{5}$$

where $\mathcal{A}$ is the electric-field component of the fundamental ML solution of Eqs. (1)–(3) with $\eta = 0$ (free running laser); T_r is the period of the ML solution, $T_r \approx T$; $\psi_1^\dagger$ is the "phase-shift" neutral mode of the linear operator adjoint to the operator that describes stability of the fundamental ML solution of the free running laser. w_h in Eq. (4) is the asymptotic half-width of the locking cone.

Expression (4) is valid for small values of η only. However, this should not be considered as a major restriction, since minimal values of injection strength should be used in experiments in order to avoid a suppression of the ML regime by injection and minimize its effect on the pulse shape. A similar expression can be derived for the half-width of the locking cone of a noncentral mode. In the next section, we study numerically the dependence of the asymptotic half-width of the locking cone defined by formula (5) on the laser parameters and compare the results obtained using this formula with those of direct numerical integration of Eqs. (1)–(3). The injection power parameter η^2 used in the direct integration of Eqs. (1)–(3) was of the same order as the power of the central mode of the ML solution, which agrees with typical experimental setting.

The asymptotic expressions (4) and (5) are obtained under the assumption that $\alpha_{g,q} = 0$. This assumption simplifies the numerical calculation of the adjoint neutral mode $\psi^\dagger = \psi_1^\dagger$, which enters the r.h.s. of Eq. (5). In the absence of injection, the linear operator L describing the stability of the ML solution has two neutral modes, one corresponding to the phase-shift invariance of the model equations and the other corresponding to the invariance with respect to arbitrary time shifts. Similarly, apart from the "phase-shift" neutral mode $\psi^\dagger$, the adjoint operator $L^\dagger$ has a second "translational" neutral mode $\chi^\dagger$ related to the time-shift invariance of the model (see Appendix for details). In the case of zero α factors in the gain and absorber sections, the calculation of the adjoint "phase-shift" neutral mode $\psi^\dagger$ is rather simple: it is a solution of a scalar linear-delay differential equation obtained by separating the imaginary part of the field equation of the adjoint linear problem from its real part, the gain, and the loss equation [Sec. A2, formulas (A7) and (A9)]. On the contrary, when at least one of the two α factors is nonzero, both the adjoint neutral modes, $\psi^\dagger$ and $\chi^\dagger$, should be determined simultaneously by solving a system of four coupled equations.

Formulas (4) and (5) describe the locking range of a CW solution of Eqs. (1)–(3) as well. In this case, $\mathcal{A} = A_0 = \text{const}$, $\psi_1^\dagger = \text{const}$, and the formula transforms into $|\omega|/\eta \leqslant \gamma(1+\gamma T)^{-1}/A_0$. This agrees with the asymptotic locking range estimate $|\omega|/\eta \leqslant 1/A_0$ for a standard single-mode laser model. This latter model can be derived from Eqs. (1)–(3) by

setting $\gamma = \infty$, $T = 1$, and expanding nonlinear terms, see Ref. [11].

III. NUMERICAL RESULTS

The analysis of the impact of laser parameters on the width of the locking cone has been performed by numerical calculation of w_h in the inequality (4). The comparison of the results of these calculations with those of direct numerical integration of the model equations indicates that the accuracy of the asymptotic relation (4) depends strongly on the stability properties of the ML solution. We have found that the discrepancy between the values of the half-width of the locking cone obtained by the asymptotic formula (5) and by the direct integration of the model is less than 3% when the ML solution satisfies New's background stability criterion; i.e., the net gain parameter is negative,

$$G(t) - Q(t) + \ln\kappa < 0, \tag{6}$$

between two successive ML pulses where the electric field intensity is close to zero [6,19]. Physically New's criterion means that small perturbations of the low-intensity background between ML pulses decay with time (absolute stability). As it was demonstrated in Ref. [6], close to the instability boundary of the fundamental ML solution, stable pulses that do not satisfy New's criterion can exist. According to our results, expressions (4) and (5) do not provide an accurate estimate of the locking cone for such ML pulses. We illustrate this fact with Fig. 5, where the half-width of the locking cone estimated using formula (5) (solid line) is compared to that obtained by direct simulation of Eqs. (1)–(3) (dotted line). One can see that for $\gamma_q > 0.95$, asymptotic results differ from those obtained by direct numerical simulations. This discrepancy is related to the fact that for the chosen parameter values, New's criterion is satisfied for $\gamma_q < 0.95$. For $\gamma_q > 0.95$, Eqs. (1)–(3) have a stable ML solution, but the locking cone calculated by means of direct numerical integration of the model equations appears to be wider than that estimated using expressions (4) and (5).

The absorber relaxation rate γ_q increases with the absolute value of the reverse voltage applied to the absorber section.

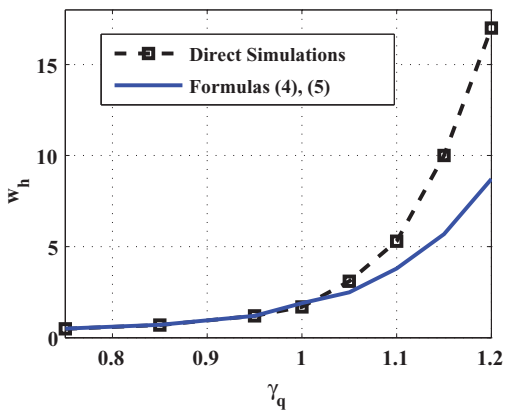

FIG. 5. (Color online) Dependence of the half width of the locking cone on γ_q: direct integration (dashed line) and estimate obtained by formulas (4) and (5) (solid line). $T = 2.5$, $\gamma = 30$, $\kappa = 0.1$, $g_0 = 1$, $q_0 = 2$, $\gamma_g = 0.01$, $s = 25$.

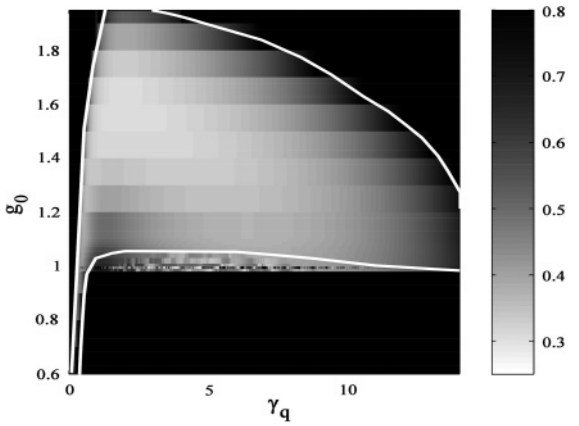

FIG. 6. Dependence of the half width of the locking cone on γ_q and g_0 obtained using formulas (4) and (5). $T = 2.5$, $\gamma = 30$, $\kappa = 0.1$, $q_0 = 4$, $\gamma_g = 0.01$, $s = 25$.

Hence, for the study of the impact of the absorber bias on the locking cone width, we vary the parameter γ_q. The two-parametric plot in Fig. 6 illustrates the dependence of the asymptotic half-width of the locking cone on the gain parameter g_0 and the relaxation rate γ_q in the absorbing section, with the fixed unsaturated absorption parameter q_0. Color intensity represents the width of the locking cone and white lines show the boundaries of the domain where periodic ML pulses are stable and satisfy New's criterion. Within the region bounded by the white lines, asymptotic expressions (4) and (5) give an estimate of the locking cone width with 3% accuracy. Crossing the lower left or right boundaries of this region leads to a break-up of the periodic ML regime and results in a modulated output, shown in Fig. 3. In particular, in the black area located between the vertical axis $\gamma_q = 1$ and the white line, the peak power of the ML regime is modulated with the Q-switching frequency [see Fig. 3(b)]. Above the the region bounded by the white lines, we have observed stable periodic ML pulses. However, they do not satisfy New's criterion and

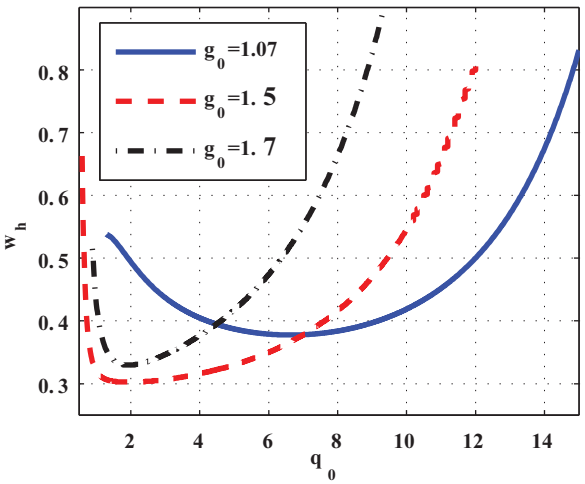

FIG. 7. (Color online) Dependence of the half width of the locking cone on γ_q computed using formulas (4) and (5). $T = 2.5$, $\gamma = 30$, $\kappa = 0.1$, $q_0 = 4$, $\gamma_g = 0.01$, $s = 25$.

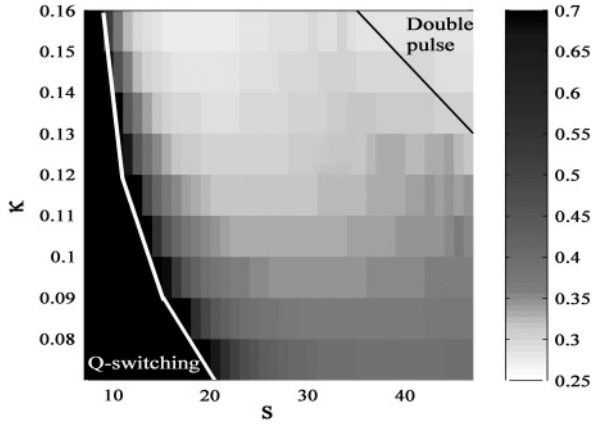

FIG. 8. Dependence of the half width of the locking cone on κ and s obtained using formulas (4) and (5). $T = 2.5$, $\gamma = 30$, $g_0 = 1$, $q_0 = 2$, $\gamma_g = 0.01$.

the results obtained with formula (5) diverge from the results of direct integration of the model.

Figure 6 shows that the half-width of the locking cone increases near the boundary where New's criterion for a stable ML regime is violated. This trend is more clearly illustrated by Fig. 7, which shows three one-parametric cross sections of the plot in Fig. 6.

The ML pulses satisfying New's criterion can exist only provided that the absorbing medium is saturated faster than the gain medium, i.e., when $s > 1$, see for example Ref. [19] for details. When gain and loss per cavity round trip are not small, such pulses are possible only if a more strict condition $s\kappa > 1$ is satisfied [6,11].

Figures 8 and 9 present the dependence of the asymptotic half-width of the locking cone on the parameters κ and s. The domain where the stable periodic ML regime satisfies New's criterion is bounded by the black and white lines in the two-parametric plot in Fig. 8. The left boundary corresponds to the violation of New's criterion and almost immediate transition to the Q-switched ML state. The right boundary corresponds to the transition to a harmonic ML state with two coexisting pulses in the laser cavity. The one-parametric plots in Fig. 9, showing three cross sections of the plot in Fig. 8, indicate that the half-width of the locking cone increases toward the

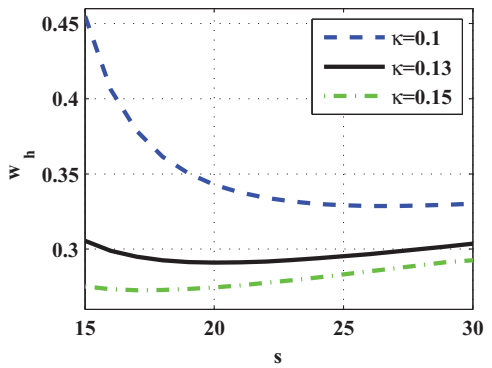

FIG. 9. (Color online) Dependence of the half width of the locking cone on s obtained using formulas (4) and (5). $T = 2.5$, $\gamma = 30$, $g_0 = 1$, $q_0 = 2$, $\gamma_g = 0.01$.

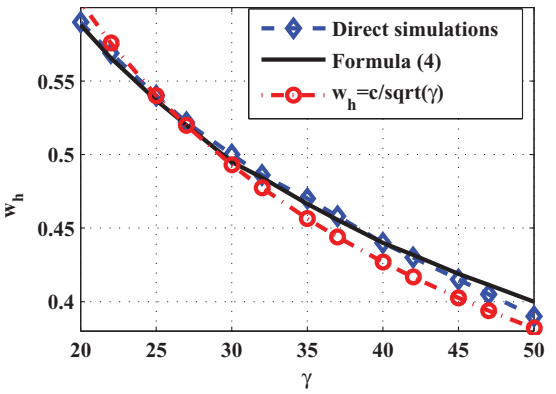

FIG. 10. (Color online) Dependence of the half width of the locking cone on γ obtained using formulas (4) and (5) (solid line), direct simulations (dashed line), and fitted curve $w_h = \frac{c}{\sqrt{\gamma}}$ (dot-dashed line). $T = 2.5$, $\kappa = 0.1$, $g_0 = 1$, $q_0 = 2$, $\gamma_g = 0.01$, $\gamma_q = 0.75$, $s = 25$.

boundaries of the domain of stable ML operation; i.e., they demonstrate the same trend as Figs. 6 and 7. Figure 9 also shows that the locking cone becomes wider with the increase of linear nonresonant intensity losses, i.e., when the attenuation factor κ decreases.

As it is shown in the Appendix, for large γT, expression (5) can be further simplified to

$$w_h = \frac{c}{\sqrt{\gamma}}; \tag{7}$$

see Sec. A3 for details and discussion of the constant c. The results of direct numerical integration of model equations (1)–(3), shown in Fig. 10, indicate that, in agreement with the asymptotic formula (7), the width of the locking cone scales with increasing γ as $\gamma^{-1/2}$. Hence, the locking cone becomes more narrow when the number of ML modes increases and the pulse becomes shorter. Therefore, one can expect that, in some situations, incorporating an additional spectral filtering section into the laser cavity would help to increase the locking range. This is in agreement with the results obtained for a hybrid ML laser [20]. On the other hand, experimental data indicate that the increase of the bandwidth results in shortening of the pulse to a certain limit only, after which the width of the pulse does not change when the spectrum becomes wider, suggesting that the synchronization of side modes becomes rather poor. This effect is not present in models (1)–(3); it can be possibly taken into account by including additional terms such as noise sources.

IV. CONCLUSIONS

Using a delay-differential model of a passively mode-locked semiconductor laser with a single-frequency coherent optical injection, we have shown that the asymptotic analysis gives a good approximation of the locking-cone boundaries provided that (a) the intensity of the injected light is sufficiently small (we used the ratio of the single-mode injection to output intensity typical of experimental setting); and (b) parameters of the laser ensure generation of ML pulses with "stable background" as defined by New's criterion [6]. In our calculations, formulas (4) and (5) give approximation of

the locking boundaries with error less than 3% for parameters within the domain where the stable periodic fundamental ML solution satisfies New's criterion. We have used the asymptotic formula (4) to study the dependence of the width of the locking cone on laser parameters. In particular, we have demonstrated that the width of the locking cone increases when parameters approach the boundaries of stable ML operation of the free-running laser. In short, the less stable the ML regime, the wider the locking cone.

An asymptotic approach similar to that used to derive formula (4) can be applied for the estimation of the locking cone width in a passively ML laser with two-frequency coherent optical injection, such as the lasers studied experimentally in Ref. [4], and in a hybrid ML laser [20], as well as for studying the effect of small noise on ML operation.

ACKNOWLEDGMENTS

The authors acknowledge the support of EU FP7 Initial Training Network PROPHET (Grant No. 264687). A.V. acknowledges the support of SFB Project 787 of the DFG and the "Research and Pedagogical Cadre for Innovative Russia" program (Grant No. 2011-1.5-503-002-038).

APPENDIX

1. Analysis with the method of two time scales

Here we derive the asymptotic formulas (4) and (7) using the method of multiple time scales.

To shorten the notation, we rewrite Eqs. (1)–(3) with $\alpha_{g,q} = 0$ as

$$\gamma^{-1}\frac{dA}{dt} + A = \sqrt{\kappa}e^{(G_T - Q_T)/2}A_T + \varepsilon\eta e^{i\varepsilon\omega t},$$
$$\frac{dH}{dt} = F(H, |A|^2), \tag{A1}$$

where H stands for (G, Q) and a small parameter ε is introduced; hence, η and ω are of order $O(1)$. We further introduce the time scales $\tau_0 = t$ and $\tau_1 = \varepsilon t$ with the corresponding operators of differentiation $D_0 = \frac{\partial}{\partial\tau_0}$ and $D_1 = \frac{\partial}{\partial\tau_1}$ and look for solutions of Eqs. (1)–(3) in the form $A = A^0 + \varepsilon A^1, G = G^0 + \varepsilon G^1$, $Q = Q^0 + \varepsilon Q^1$, where each term is a function of the two times, for example, $A(\tau_0, \tau_1) = A^0(\tau_0, \tau_1) + \varepsilon A^1(\tau_0, \tau_1)$ and $\frac{dA}{dt} = D_0 A + \varepsilon D_1 A$.

After expanding Eq. (A1) with respect to ε and separating order $O(1)$ terms from $O(\varepsilon)$ terms, while neglecting the terms of higher order, we arrive at the system

$$\gamma^{-1}D_0 A^0 + A^0 = \sqrt{\kappa}e^{(G_T^0 - Q_T^0)/2}A_T^0,$$
$$D_0 H^0 = F(H^0, |A_0|^2) \tag{A2}$$

for the leading order terms $A^0, H^0 = (G^0, Q^0)$ and the equations

$$\gamma^{-1}D_0 A^1 + A^1 + \gamma^{-1}D_1 A^0$$
$$= \eta e^{i\omega\tau_1} + \sqrt{\kappa}e^{(G_T^0 - Q_T^0)/2}\big(A_T^1 - T D_1 A_T^0 + A_T^0\big(G_T^1 - Q_T^1\big)$$
$$- \tfrac{1}{2}T D_1\big(G_T^0 - Q_T^0\big)\big),$$
$$D_0 H^1 + D_1 H^0 = F_H'(H^0, |A^0|^2)H^1$$
$$+ F_I'(H^0, |A^0|^2)(A^0(A^1)^* + (A^0)^* A^1), \tag{A3}$$

for the corrections $A^1, H^1 = (G^1, Q^1)$, where F_H' is the Jacobian matrix of F with respect to H; F_I' is the partial derivative of F with respect to $I = |A|^2$; and the asterisk denotes the complex conjugate; only the time τ_0 is retarded in the delayed terms; i.e., for example, $A_T^0 = A^0(\tau_0 - T, \tau_1)$. The solution of the leading order Eq. (A2) is

$$A^0 = e^{i\varphi(\tau_1)}\mathcal{A}(\tau_0 + \theta(\tau_1)), \quad H^0 = \mathcal{H}(\tau_0 + \theta(\tau_1)), \tag{A4}$$

where $(\mathcal{A}, \mathcal{H}) = (\mathcal{A}, \mathcal{G}, \mathcal{Q})$ is the ML solution of the free-running laser system with the real-valued field component $\mathcal{A}$ starting at some distinguished moment, for example, at the maximum of $\mathcal{A}$. It is convenient to shift the time and phase in the correction A^1, H^1 similarly, i.e., to replace $A^1(\tau_0, \tau_1)$ with $e^{i\varphi(\tau_1)}A^1(\tau_0 + \theta(\tau_1), \tau_1)$. Then, substituting Eq. (A4) into Eq. (A3), and using the fact that $(\mathcal{A}, \mathcal{H})$ solves the free-running laser equations, we obtain the system for A^1, H^1,

$$\gamma^{-1}D_0 A^1 + A^1 - \sqrt{\kappa}e^{(\mathcal{G}_T - \mathcal{Q}_T)/2}\big(A_T^1 + \mathcal{A}_T\big(G_T^1 - Q_T^1\big)/2\big)$$
$$= -i\varphi' T(\gamma^{-1}\dot{\mathcal{A}} + \mathcal{A} + (\gamma T)^{-1}\mathcal{A})$$
$$- \theta' T(\gamma^{-1}\ddot{\mathcal{A}} + \dot{\mathcal{A}} + (\gamma T)^{-1}\dot{\mathcal{A}}) + \eta e^{i(\omega\tau_1 - \varphi)},$$
$$D_0 H^1 - F_H'(\mathcal{H}, \mathcal{I})H^1 - F_I'(\mathcal{H}, \mathcal{I})\mathcal{A}((A^1)^* + A^1) = -\theta'\dot{\mathcal{H}}, \tag{A5}$$

where $\mathcal{I} = \mathcal{A}^2$ and $\mathcal{A}, \dot{\mathcal{A}} = \frac{d\mathcal{A}}{d\tau_0}, \ddot{\mathcal{A}} = \frac{d^2\mathcal{A}}{d\tau_0^2}, \mathcal{H}, \dot{\mathcal{H}} = \frac{d\mathcal{H}}{d\tau_0}$ are functions of τ_0, and $\varphi' = \frac{d\varphi}{d\tau_1}$, $\theta' = \frac{d\theta}{d\tau_1}$ are functions of τ_1.

Now, employing the general approach of the method of multiple time scales, we derive equations for the evolution of the slow variables φ, θ from the solvability conditions for system (A5) with respect to (A^1, H^1) under periodic boundary conditions in τ_0. The l.h.s. of Eq. (A5) is the linearization of Eqs. (1)–(3) with $\eta = 0$ (the free-running laser equations) on the ML solution. This linearization has a two-dimensional space of periodic solutions corresponding to the two symmetries of the free-running laser equations, one with respect to time shifts, the other with respect to phase shifts (rotations of the complex A plane); the periodic eigenfunctions of the linearization corresponding to the phase shift and the time shift, respectively, are

$$\psi = (i\mathcal{A}, 0, 0)^T, \quad \chi = (\dot{\mathcal{A}}, \dot{\mathcal{G}}, \dot{\mathcal{Q}})^T, \tag{A6}$$

where the superscript T denotes the transposition. Hence, the adjoint linear system has a two-dimensional space of periodic solutions, too (this system is considered in the next subsection in more detail). We denote by $\psi^\dagger, \chi^\dagger$ the linearly independent pair of the adjoint periodic solutions defined by the normalization conditions

$$\langle\psi^\dagger, \psi\rangle = \langle\chi^\dagger, \chi\rangle = 1, \quad \langle\psi^\dagger, \chi\rangle = \langle\chi^\dagger, \psi\rangle = 0,$$

with the inner product

$$\langle u, v\rangle = \mathrm{Re}\left(\int_0^{T_r}(u(t))^T(v(t))^* dt\right),$$

where T_r is the period of the ML solution $(\mathcal{A}, \mathcal{G}, \mathcal{Q})$. As discussed in the next subsection, the adjoint functions have the form

$$\psi^\dagger = (i\psi_1^\dagger, 0, 0)^T, \quad \chi^\dagger = (\chi_1^\dagger, \chi_2^\dagger, \chi_3^\dagger)^T, \tag{A7}$$

where both $\psi_1^\dagger$, $\chi_1^\dagger$ are real-valued, i.e., similarly to ψ, the adjoint function $\psi^\dagger$ has purely imaginary A component and zero G,Q components, while the adjoint function $\chi^\dagger$ has the real A component like χ.

According to the Fredholm alternative, system (A5) with the periodic boundary conditions in τ_0 is solvable if the r.h.s. of this system, as a function of τ_0, is orthogonal to each of the adjoint functions $\psi^\dagger = \psi^\dagger(\tau_0), \chi^\dagger = \chi^\dagger(\tau_0)$ for each τ_1. Using expressions (A7), one can write this solvability criterion in the form of the system

$$\varphi' = k_1\eta\sin(\omega\tau_1 - \varphi), \quad \theta' = k_2\eta\cos(\omega\tau_1 - \varphi), \tag{A8}$$

with

$$k_1 = w_h,$$

where w_h defined by formula (5), and

$$k_2 = \frac{\int_0^{T_r}\chi_1^\dagger(t)\,dt}{\int_0^{T_r}(T\chi_1^\dagger(\gamma^{-1}\ddot{\mathcal{A}} + \dot{\mathcal{A}} + (\gamma T)^{-1}\mathcal{A}) + \chi_2^\dagger\dot{\mathcal{G}} + \chi_3^\dagger\dot{\mathcal{Q}})\,dt}.$$

Adler's type equations (A8) define dynamics of the slow variables φ,θ. In particular, the LML regime is determined by the criterion

$$\varphi' = \omega, \quad \theta' = \text{const}.$$

Hence, for the LML solution, $\varphi = \omega\tau_1 + \varphi_0$, and due to the first of equations (A8), $\omega = -k_1\eta\sin\varphi_0$, consequently,

$$|\omega| \leqslant k_1\eta = w_h\eta,$$

i.e., formula (4) holds.

2. Adjoint functions

Let us introduce the notation $J = \operatorname{Im} A$, $R = \operatorname{Re} A$, $A = (J,R)$ and replace the complex A Eq. (1) in Eqs. (1)–(3) with the pair of real equations. Consider the Jacobian matrix B of the r.h.s. of the free-running laser equations ($\eta = 0$) with respect to the variables J,R,G,Q and the Jacobian matrix C with respect to the delayed variables J_T,R_T,G_T,Q_T. Evaluating these matrices on the ML solution $(0,\mathcal{A},\mathcal{G},\mathcal{Q})$, we obtain T_r-periodic matrices $\mathcal{B}$ and $\mathcal{C}$, respectively. The periodic eigenfunctions (A6), which in the real notation of this section have the form $\psi = (\mathcal{A},0,0,0)$, $\chi = (0,\dot{\mathcal{A}},\dot{\mathcal{G}},\dot{\mathcal{Q}})$, solve the system

$$\dot{z} = \mathcal{B}(t)z + \mathcal{C}(t-T)z(t-T).$$

The adjoint functions $\psi^\dagger$, $\chi^\dagger$ solve the adjoint system

$$\dot{y} = -\mathcal{B}^T(t)y - \mathcal{C}^T(t+T)y(t+T),$$

see, e.g., Ref. [21]. The explicit computation of the matrices $\mathcal{B}$, $\mathcal{C}$ shows that the first equation in each of these systems separates from the other three equations. Hence, $\psi^\dagger = (\psi_1^\dagger,0,0,0)^T$, $\chi^\dagger = (0,\chi_1^\dagger,\chi_2^\dagger,\chi_3^\dagger)^T$ [cf. Eq. (A7)], where $\psi_1^\dagger$ is a nontrivial periodic solution of the scalar equation

$$\dot{\psi}_1^\dagger = \gamma\psi_1^\dagger - \frac{\dot{\mathcal{A}}(t+T) + \gamma\mathcal{A}(t+T)}{\mathcal{A}(t)}\psi_1^\dagger(t+T), \tag{A9}$$

and $(\chi_1^\dagger,\chi_2^\dagger,\chi_3^\dagger)^T$ is a nontrivial periodic solution of the system

$$\begin{aligned}
\dot{\chi}_1^\dagger &= \gamma\chi_1^\dagger + 2e^{-\mathcal{Q}}(e^{\mathcal{G}}-1)\mathcal{A}\chi_2^\dagger + 2s(1-e^{-\mathcal{Q}})\mathcal{A}\chi_3^\dagger \\
&\quad - \frac{\dot{\mathcal{A}}(t+T) + \gamma\mathcal{A}(t+T)}{\mathcal{A}(t)}\chi_1^\dagger(t+T), \\
\dot{\chi}_2^\dagger &= (\gamma_g + e^{\mathcal{G}-\mathcal{Q}}\mathcal{A}^2)\chi_2^\dagger - \frac{\dot{\mathcal{A}}(t+T) + \gamma\mathcal{A}(t+T)}{2}\chi_1^\dagger(t+T), \\
\dot{\chi}_3^\dagger &= -e^{-\mathcal{Q}}(e^{\mathcal{G}}-1)\mathcal{A}^2\chi_2^\dagger + (\gamma_q + se^{-\mathcal{Q}}\mathcal{A}^2)\chi_3^\dagger \\
&\quad + \frac{\dot{\mathcal{A}}(t+T) + \gamma\mathcal{A}(t+T)}{2}\chi_1^\dagger(t+T).
\end{aligned}$$

The nonzero component $\psi_1^\dagger$ of the adjoint function $\psi^\dagger$ can be easily found numerically by solving Eq. (A9) in the reverse time as, after the time reversion, this equation becomes stable. The same is true for the function $\chi^\dagger$.

3. Dependence of the locking cone on γ

Assume that $\gamma \gg 1$, T is fixed and the ML solution of the free-running laser equations scales with γ as in the Haus limit, i.e., the period of the ML solution scales as

$$T_r = T + \gamma^{-1}\delta, \tag{A10}$$

and the electric-field envelope $\mathcal{A}$ is very close to zero between the pulses, while during the pulse

$$\mathcal{A}(t) = \sqrt{\gamma}a(\gamma t) \tag{A11}$$

(note that in the Haus model $a = \operatorname{sech}$). Then, the periodic solution $\psi_1^\dagger$ of the adjoint Eq. (A9) is also a periodic sequence of pulses that are synchronized with the pulses of $\mathcal{A}$. Using the periodicity of $\mathcal{A}$ and $\psi_1^\dagger$ with the common period T_r and the scaling relation (A10), we rewrite Eq. (A9) as

$$\dot{\psi}_1^\dagger = \gamma\psi_1^\dagger - \frac{\dot{\mathcal{A}}(t-\gamma^{-1}\delta) + \gamma\mathcal{A}(t-\gamma^{-1}\delta)}{\mathcal{A}(t)}\psi_1^\dagger(t-\gamma^{-1}\delta).$$

On the fast stage (i.e., during the pulse), using the ansatz (A11) and introducing the fast-time $\tau = \gamma t$, we obtain

$$\dot{\psi}_1^\dagger = \psi_1^\dagger - \frac{\dot{a}(\tau-\delta) + a(\tau-\delta)}{a(\tau)}\psi_1^\dagger(\tau-\delta).$$

Hence, on the fast stage, $\psi_1^\dagger$ scales with γ in the same way as $\mathcal{A}$ does, namely, $\psi_1^\dagger(t) = \phi(\gamma t)$, where ϕ is a positive solution of the problem

$$\dot{\phi} = \phi - \frac{\dot{a}_\delta + a_\delta}{a}\phi_\delta, \quad \phi(-\infty) = \phi(\infty) = 0.$$

Therefore, in the limit of large γ, the asymptotic formula (4) can be rewritten as (7) with

$$c = \frac{\int_{-\infty}^{\infty}\phi(\tau)\,d\tau}{T\int_{-\infty}^{\infty}\phi(\tau)(\dot{a}(\tau)+a(\tau))\,d\tau}.$$

[1] P. J. Delfyett, S. Gee, M.-T. Choi, H. Izadpanah, W. Lee, S. Ozharar, F. Quinlan, and T. Yilmaz, J. Lightwave Technol. **24**, 2701 (2006).
[2] M. Kuramoto, N. Kitajima, H. Guo, Y. Furushima, M. Ikeda, and H. Yokoyama, Opt. Lett. **32**, 2726 (2007).
[3] N. Rebrova, T. Habruseva, G. Huyet, and S. P. Hegarty, Appl. Phys. Lett. **97**, 101105 (2010).
[4] T. Habruseva, S. O'Donoghue, N. Rebrova, D. A. Reid, L. P. Barry, D. Rachinskii, G. Huyet, and S. P. Hegarty, IEEE Photonics Technol. Lett. **22**, 359 (2010).
[5] F. Mogensen, H. Olesen, and G. Jacobsen, IEEE J. Quantum Electron. **QE-21**, 784 (1985).
[6] A. G. Vladimirov and D. Turaev, Phys. Rev. A **72**, 033808 (2005).
[7] A. G. Vladimirov, D. Turaev, and G. Kozyreff, Opt. Lett. **29**, 1221 (2004).
[8] A. G. Vladimirov and D. Turaev, Radiophys. Quantum Electron. **47**, 769 (2004); **47**, 10 (2004).
[9] H. Haus, IEEE J. Quantum Electron. **QE-11**, 736 (1975).
[10] H. Haus, IEEE J. Sel. Top. Quantum Electron. **6**, 1173 (2000).
[11] D. Rachinskii, A. G. Vladimirov, U. Bandelow, B. Huettl, and R. Kaiser, J. Opt. Soc. Am. B **23**, 663 (2006).
[12] E. A. Viktorov, P. Mandel, A. G. Vladimirov, and U. Bandelow, Appl. Phys. Lett. **88**, 201102 (2006).
[13] A. G. Vladimirov, A. S. Pimenov, and D. Rachinskii, IEEE J. Quantum Electron. **45**, 462 (2009).
[14] A. G. Vladimirov, U. Bandelow, G. Fiol, D. Arsenijevic, M. Kleinert, D. Bimberg, A. Pimenov, and D. Rachinskii, J. Opt. Soc. Am. B **27**, 2102 (2010).
[15] M. Nizette, D. Rachinskii, A. G. Vladimirov, and M. Wolfrum, Physica D **218**, 95 (2006).
[16] K. Engelborghs, T. Luzyanina, and D. Roose, ACM Trans. Math. Software **28**, 1 (2002).
[17] J. Guckenheimer and P. Holmes, *Nonlinear Oscillations, Dynamical Systems and Bifurcations of Vector Fields* (Springer, London, 1983).
[18] S. Wieczorek, Thomas B. Simpson, B. Krauskopf, and D. Lenstra, Opt. Commun. **215**, 125 (2003).
[19] G. H. C. New, IEEE J. Quantum Electron. **10**, 115 (1974).
[20] A. G. Vladimirov, M. Wolfrum, G. Fiol, D. Arsenijevic, D. Bimberg, E. Viktorov, P. Mandel, and D. Rachinskii, Proc. SPIE **7720**, 77200Y-1-8 (2010).
[21] A. Halanay, *Differential Equations; Stability, Oscillations, Time Lags* (Academic Press, New York, 1966).